Self-diffusion of Nanoscale particles with hard and soft sphere models

Huawei Sun[1] · **Yaohong Wang**[1]

Contact: yaohong@tju,edu.cn
Center for Applied Mathematics, Tianjin University, Tianjin, 300073, China

Abstract
The diffusion of particles in suspension is investigated by a thermostat based on fluctuating hydrodynamics for dynamic simulations of implicit-solvent coarse-grained model which can take into account both hydrodynamic and Brownian effects. Particles with cut-and-shifted Lennard-Jones and Gaussian-core potential are studied. The results show that their diffusion process can be characterized by three regimes: ballistic motion, short-time diffusion and long-time diffusion. We observe that the mean square displacement (*MSD*) of regime I, ballistic motion, is proportional to t^2. For the other two regimes, its *MSD* is proportional to t with different slopes. Furthermore, we study the diffusion coefficients of spherical particles from *MSD* at different volume fractions. For the cut-and-shifted Lennard-Jones potential model, we observe the diffusion coefficients decrease monotonously with the increase of volume fraction (0.02-0.3), and consistent with the results of the experiment. However, for the Gauss-core potential model, the curve of long-time self-diffusion coefficient as a function of dimensional density (0.001 to 1) appears to be nonmonotonic. It shows that the long-time self-diffusion coefficient decreases monotonically when the dimensional density is below 0.3, and then increases anomalously when the dimensionless density passes through 0.3.

Keywords: Brownian Motion · Nanoparticles · Self-diffusion · Suspensions

1. Introduction

Diffusion of particles in suspensions is widely encountered in nature and science, for example the silica nanoparticles in polyethylene glycol [1], polymer coils in solution [2], dendrimer solutions [3-6] and protein solution [7,8], polystyrene nanoparticles [9]. The investigation of diffusion of particles in suspensions must take into account both hydrodynamic and Brownian effects. A variety of studies on diffusion can be found in the literature; there have been experimental work [7,11-12], analytical work [12-14], and numerical work on studying diffusion.

The diffusion of particles in suspension will also be affected by the interaction between particles. And there are different types of particles, in particular hard and soft. A cut-and-shifted Lennard-Jones potential model, proposed by Week, Chandler, and Andersen[15], known as *WCA* potential, is introduced to study hard particles, which is impossible to overlap between particles, for example biological bacteria [16,17], macromolecular protein [7], nanomaterials et al. For soft particles, Stillinger [18] in 1976 proposed Gaussian-core potential [19–22], in which interaction between particles is given by the Gaussian potential and particles may overlap with each other. With Gaussian-core potential models, we obtain the dynamic anomalous behaviour of the soft particle system compared with hard sphere models.

The diffusion coefficient of a single spherical particle in infinitely diluted suspension for Brownian motion is characterized by Stokes-Einstein relation [23]. However, this result is not applicable in high concentration suspension or near boundary wall cases. For a single particle in dense suspension, the fluid field around it would be driven by the movement of nearby particles. One may expect, as the suspension becomes denser, the particles diffusivity goes more complex. Additionally, the viscosity of suspension will be also affected by the interaction or the aggregation of particles [24]. Hence the study of Brownian particles in different volume fractions becomes necessary.

Segrè [25] studied the short-time diffusion of particles suspended in a liquid by simulations based on the fluctuating Lattice Boltzmann method. Heinen [26] and Banchio [27] reported the short-time dynamics of charged colloidal spheres by accelerated Stokesian dynamics and Brownian dynamics simulation, where the interaction between particles is given by a hard sphere plus repulsive Yukawa pair potential. Napoli et al. [9] investigated the effects of channel, ionic and pH value on the diffusivity of spherical particles by experimental method. Ando et al. studied the effect of macromolecular shape and importance of hydrodynamic interaction on diffusion by

Brownian dynamics [28]. And there are also many other numerical methods which can be used to study the importance of hydrodynamic interaction on the dynamics of colloidal suspensions, such as multi- particle collision dynamics [29], Stokesian dynamics [30] and dissipative particle dynamics [31] and molecular dynamics [7]. Beenakker and Mazur [12, 13] presented a theory about the short-time self-diffusion coefficient as a function of volume fraction, where the hydrodynamic interaction between an arbitrary number of spherical particles are taken into account. Hoh and Zia [14] studied the contributions of hydrodynamic, Brownian and interparticle to the self-diffusion respectively through theoretical analysis. There are also many other theoretical works that can study Brownian motion, such as dynamical density functional theory [32], and mode-coupling theory [19].

The paper is organized as follows: Section 2 describes the mathematical formulation of the problem using the Stochastic Eulerian Lagrangian Methods [33] and the hard and soft sphere models. Results of simulation are discussed in Section 3. The final section will be devoted to summarize the article and provide an outlook.

2. Methodology

Diffusion characteristics of nanoscale particles in suspension are simulated by the Stochastic Eulerian Lagrangian Method (SELM) which is developed by the following: the interaction force between the particles is calculated by the molecular dynamics software LAMMPS [34]. Secondly, the interaction between particles and fluid is derived from the immersed boundary method [35]. Finally, Brownian motion of the particles is modelled by introducing thermal force.

The particle in an incompressible fluid flow satisfies the following equations:

$$\nabla \cdot \boldsymbol{u} = 0, \tag{1.1}$$

$$\rho_l \frac{\partial \boldsymbol{u}}{\partial t} = \mu \nabla^2 \mathrm{u} + \Lambda[\Upsilon(\mathrm{v} - \Gamma \mathrm{u})] - \nabla p + \mathrm{f}_{thm}, \tag{1.2}$$

$$m \frac{d\boldsymbol{v}}{dt} = -\Upsilon(\boldsymbol{v} - \Gamma \boldsymbol{u}) - \nabla_x \Phi(\boldsymbol{X}) + \mathrm{F}_{thm} \tag{1.3}$$

$$\frac{d\boldsymbol{X}}{dt} = \boldsymbol{v} \tag{1.4}$$

where the simulation domain is [$-L_x/2$, $L_x/2$]×[$-L_y/2$, $L_y/2$] ×[$-L_z/2$, $L_z/2$] with periodic boundary. The velocity and the pressure of the solvent fluid is denoted by $\boldsymbol{u}$ and p. The $\boldsymbol{X}$, $\boldsymbol{v}$ denotes positions and velocities of the particles. The m, ρ_l, μ and Φ are the mass of the particles, the mass density of the solvent, the shear viscosity and the potential energy between particles, respectively. The operator Γ and operator Λ are provided for coupling structure and fluid dynamics, and Υ serves to calculate the drag force when the velocity is different between the microstructure and the surrounding fluid $\Upsilon \boldsymbol{v} = 6\pi\mu R\boldsymbol{v}$, where R is the radius of spherical particle.

Thermal forces $\mathbf{f}_{thm}$ and $\mathbf{F}_{thm}$ are introduced by the δ-correlation Gaussian random fields with mean zero and covariances,

$$\langle \mathbf{f}_{thm}(s)\mathbf{f}_{thm}(t)^T \rangle = -2k_B T(\mu\Delta - \Lambda\Upsilon\Gamma)\delta(t-s), \tag{1.5}$$

$$\langle \mathbf{F}_{thm}(s)\mathbf{F}_{thm}(t)^T \rangle = 2k_B T\Upsilon\delta(t-s), \tag{1.6}$$

$$\langle \mathbf{f}_{thm}(s)\mathbf{F}_{thm}(t)^T \rangle = -2k_B T\Lambda\Upsilon\delta(t-s). \tag{1.7}$$

k_B and T denote Boltzmann constant and temperature, respectively. The drag force on the particles exerted by the local fluid flow is calculated by the term $-\Upsilon(\boldsymbol{v} - \Gamma\boldsymbol{u})$ through the operators Υ and Γ. The operator Λ then serves to model for the drag force how the equal-and-opposite forces exerted on the solvent are spatially distributed within the fluid body. It is important that the coupling operators satisfy the adjoint condition $\Gamma = \Lambda^*$ [36]. This adjoint condition makes sure that the dissipation occurs only through the drag Υ rather than a consequence of the interconversion operators Γ and Λ.
For thermal fluctuations, the correlation between the random drive field and its algorithm for computational generation can be also greatly simplified through this form of the adjoint condition. We will use the specific coupling operators

$$\Gamma\boldsymbol{u} = \int_\Omega \eta(\boldsymbol{y} - \boldsymbol{X}(t)\boldsymbol{u}(\boldsymbol{y},t))d\boldsymbol{y}, \tag{1.8}$$

$$\Lambda\mathbf{F} = \eta(\boldsymbol{x} - \boldsymbol{X}(t))\mathbf{F}. \tag{1.9}$$

The Peskin δ-Function given in [35] is chosen as the kernel function $\eta(\boldsymbol{x})$. This choice replaces the Dirac δ-Function to ensure that the mobility of an independent particle has a finite effective hydrodynamic radius within the fluid and behaves a good approximation of the translation invariance of the coupling compared with the discretization mesh. While other choices of the coupling operators are possible, the SELM has been shown to provide a computationally efficient method for obtaining correct far-field hydrodynamic correlations and has a well-characterized near-field interaction [33]. We refer to the coarse-grained fluctuating hydrodynamics approach given in equations (1.1)-(1.7) as SELM.

3. Results

We study the diffusion coefficients with hard sphere and soft sphere models, and the *WCA* potential model and the Gauss-core potential model are introduced to simulate these two models respectively. The simulation box is a cube with L_x=L_y=L_z=20nm. The fluid temperature is set at T = 298K and the thermal energy is given by k_BT, with the Boltzmann constant 0.008314 $(amu \cdot nm^2)/(ps^2 \cdot K)$. The fluid is assumed to be water with viscosity taken to be $602amu/(nm \cdot ps)$, and the particle density is the same as the fluid density, which is set to be $602amu/(nm^3)$.

3.1 The *WCA* Potential Model

For simulations of the hard spherical particles, the *WCA* potential between particles is introduced to prevent the particles from overlapping:

$$\begin{cases} \Phi(r) = 4\varepsilon[(\sigma/r)^{12} - (\sigma/r)^6] + \varepsilon, r < r_c \\ \Phi(r) = 0, r > r_c \end{cases}, \tag{1.10}$$

ε is equal to the depth of the potential energy well, which is fixed at $\varepsilon=k_B T$, and σ is the distance in which the interparticle potential is ε, and set to be the particle diameter, r_c is the cutoff. The values of σ and r_c are taken to be $1nm$ and $1.12nm$ respectively. Then our particle radius R is $\sigma/2=0.5nm$.

The self-diffusion of a single particle at finite volume fraction is described by three time regimes, ballistic motion, short-time diffusion and long-time diffusion, $t < \tau_n$, $t \le \tau_B$, and $t > \tau_B$. $\tau_n = m/6\pi\mu R$ is the Brownian relaxation time that characterizes short time scale from pre-Brownian ballistic regime to Brownian diffusion motion, where m is the particle mass. The time for a single particle to diffuse a distance of its radius is defined by $\tau_B = \sigma^2/D_0$, where $D_0 = k_B T/6\pi\mu R$ is the short-time self-diffusion coefficient of a single spherical particle in infinitely domain. It is a time scale when the direct interactions between surrounding particles (mainly hydrodynamics and excluded volume effect for hard particles) is more important. For $t > \tau_B$, particles move away from the cage by diffusion with a smaller slope. The latter two regimes diffusion coefficients can be obtained by the calculating the mean-square displacement as following:

$$\begin{cases} D_S = \dfrac{1}{6t}\dfrac{1}{N}\langle\sum_{i=1}^{N}(\Delta \boldsymbol{X}_i(t)\rangle, & t \le \tau_B \\ D_L = \dfrac{1}{6t}\dfrac{1}{N}\langle\sum_{i=1}^{N}(\Delta \boldsymbol{X}_i(t)\rangle, & t > \tau_B \end{cases}, \tag{1.11}$$

where $\langle\cdot\rangle$ is the ensemble average and $\Delta \boldsymbol{X}_i(t)$ is the displacement of the particle i within time t.

Initial configurations are generated by arranging particles in an orderly manner. After a long period of $8\tau_B$ with total simulation time $10\tau_B$, which is sufficient for the system to balance, the displacements data are extracted to calculate *MSD*s. Then the short-time and long-time diffusion coefficients are obtained by fitting the slopes of the *MSD* lines during 0-0.5τ_B and 1-1.5τ_B, respectively.

The three diffusion regimes are gained by analysing the *MSD*s which is reported in Fig. 1. For ballistic regime, we obtain the *MSD* result in Fig.1(a) by zooming into the initial part of the Fig.1(b). A smaller time step, $0.01ps$, is used for simulations, and we can get the *MSD* is proportional to t^2 which is consistent with the theoretical formula:

$$\langle \Delta \boldsymbol{X}(t)^2\rangle = \frac{k_B T}{m} t^2, \tag{1.12}$$

resolved from Langevin equation reported in [37]. In Fig.1(b), the time step is chosen to be $1ps$ to speed up the simulation. We can observe that there is a visible drop in the slope when the time exceeds τ_B, which shows the existence of other two regimes, short-time and long-time self-diffusion. Then the *MSD* curve can be fitted to two straight lines of different slopes that can be used to measure the diffusion coefficient of two regimes.

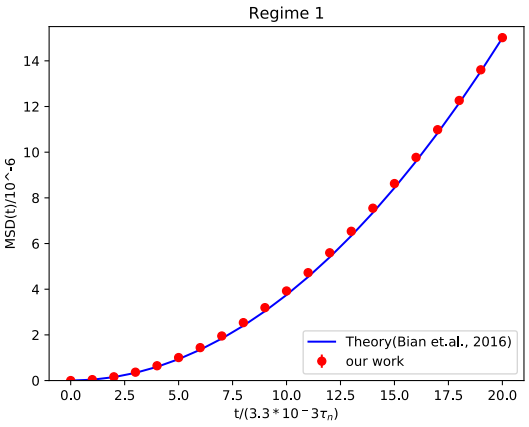

(a) Ballistic regime

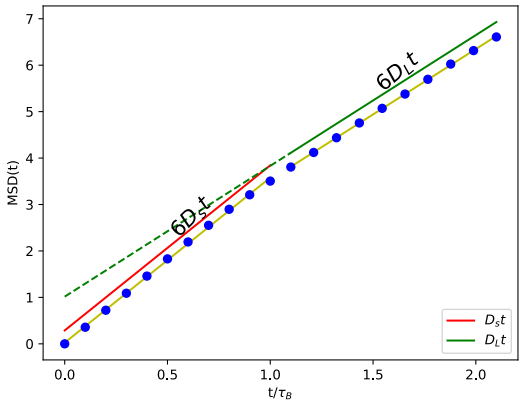

(b) Short-time and long-time self-diffusion regime

Fig. 1 Mean square displacement of the three regimes with *WCA* potential model

We also measured the short-time self-diffusion coefficients of hard spherical particles at different volume fractions ranging from 0.02 to 0.3. The number density

$$\rho = N/V, \tag{1.13}$$

where N is total particle number in suspensions, V is the volume of the simulation domain. The volume of a single particle v_{single} sever to define the volume fraction

$$\phi = v_{single}\rho = \frac{4\pi NR^3}{3V}. \tag{1.14}$$

Fig.2 depicts the *MSD* at two different volume fractions. The line of lower volume fraction has larger slope than the one of high volume fraction, which implies that the self-diffusion coefficients is indeed affected by the volume fraction.

For low volume fraction ϕ, Beenakker and Mazur [12] proposed the diffusion

$$D_s = D_0(1-1.73\phi+0.88\phi^2) \tag{1.15}$$

We compared our simulation results of normalized short-time self-diffusion coefficients as a function of volume fraction with the Langevin simulation with LAMMPS,

Beenakker and Mazur's results[12], experiments[10] and the Monte Carlo and Stokesian dynamics simulation (MCSD) [38] in Fig 3. We observed that the normalized short-time self-diffusion coefficients decrease with increasing volume fractions. As the volume fraction increases, there are more particles in the solvent. The differences between the results of the Lagenvin simulation, which is missing hydrodynamic interactions, and the others are obvious, as the particle motion is affected by the flow of solution caused by particles' movement. The hydrodynamic effects of the surrounding particles play an increased role, as the increasement of the volume fraction, and our results is in agreement with MCSD with lubrication model and experiments. Comparing to others work, the SELM naturally takes into account fully interations between the particles and the fluid.

As observed in Fig 1(b), the MSD curve slope will decrease when the time exceeds τ_B, which means that the long-time diffusion coefficient is smaller than the one of short-time regime. And we find its value also decreases as the increasement of the volume fraction, too.

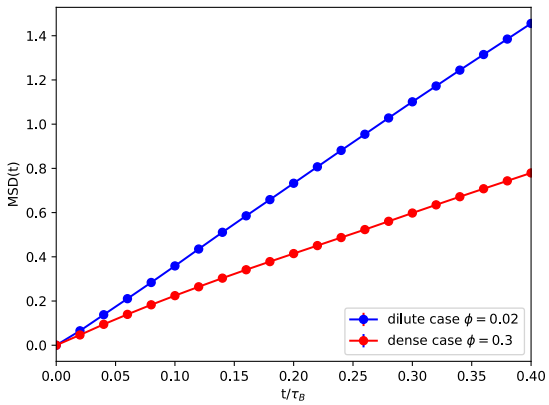

Fig. 2 Mean square displacement at low and high volume fractions

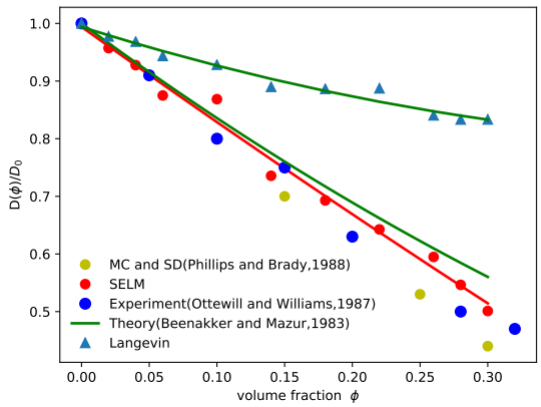

Fig. 3 Volume fraction ϕ dependence of short-time self-diffusion coefficients $D_s(\phi)/D_0$ for a suspension of hard spherical particles

3.2 The Gaussian-core Potential Model

In the case of Gaussian-core potential model, in which the pair potential of the particles is different from *WCA* potential model, is given by an ultrasoft Gaussian potential and formulated as follows:

$$\Phi(r) = \varepsilon exp[-r/\sigma], \qquad (1.16)$$

where ε is the depth of the potential energy well, which is chosen to be $\varepsilon=k_BT$. And σ is the potential range which acts as the characteristic diameter of the soft particle. The dimensionless units $T^*=k_BT/\varepsilon=0.08$ for temperature is larger than the upper freezing temperature $T^*\approx0.01$, which guarantees a stable fluid state at any density [21, 22]. Here we choose σ to be $1nm$, then the characteristic time scales τ_n and τ_B is the same as the values used in *WCA* potential case. For soft particles, we use $\rho\sigma^3$ to represent the dimensionless density of the particles, ρ is the number density defined the same as the density in equation (1.14).

Similar to the *WCA* potential model, particles are initially set in an orderly manner, and the data chosen after a long period of $8\tau_B$ with total simulation time $10\tau_B$ are used to calculate the results.

In the case of Gaussian-core potential model, three regimes of Brownian motion are also found, as shown in Fig 4, which is similar to the results of the *WCA* potential model. For ballistic regime, shown in Fig 4(a), when $t \ll \tau_n$, the *MSD* is proportional to t^2, while for diffusion regime, when time scale $t \sim \tau_B$, shown in Fig. 4(b) the *MSD* is proportional to t with two different slopes before and after time $t = \tau_B$. Compared to Fig. 1(b), the difference between short-time and long-time diffusion coefficients are smaller the *WCA* potential case.

We next study the *MSD* for different particle densities. The *MSD* diagram at $\rho\sigma^3$=0.003, 0.3, 0.6, 1.0 are shown in Fig 5. Compared to Fig 3, we can see that the diffusion coefficients are no longer decreasing monotonously as the increasement of the volume fraction. $\rho\sigma^3$=0.3 is smaller than other three cases.

To further show the relation between the diffusion coefficient and dimensionless density, we compute long time diffusion coefficient for the dimensionless density from 0.003 to 1.0, and show the results in Fig. 6. For Langevin simulation without hydrodynamic interation, the volume fraction of particles has few effects on the diffusion coefficient, and we can not catch the correct tendency as the increasement of the volume fraction. For SELM model, which takes fully account of hydrodynamic effects, we find a non-monotonic curve occurs compared to the monotonous decline of the *WCA* potential model. Mausbach and May[20] studied the diffusion coefficients of the Gaussian core model liquid by using the molecular dynamics simulation, and found the dimensionless density at the minimum diffusion coefficient was almost independent of the dimensionless temperature T^*, and its value is approximately 0.33.

In Fig. 6, we can see that the results simulated by SELM quantitatively agree with the results from their work, but smaller. What they study is a single Gauss-core potential liquid, and there is no particle plays in their model, while our model contains both the soft particles and the fluid, and the hydrodynamic effect between the particles and the fluid can reduce the diffusion of the particles. Our results show that the diffusion coefficient gradually decreases when the density $\rho\sigma^3$ is less than 0.3

and becomes minimal $0.32D_0$ at density $\rho\sigma^3$=0.3. Crossing the minimum point, the diffusion coefficient values show an anomalous increase. An obvious non-monotonic curve is characterized, which indicates that the diffusion coefficients for small densities are close to one, and the diffusion coefficient at the high density ($\rho\sigma^3$=1.0) we simulated has regained about 50% from its minimum.

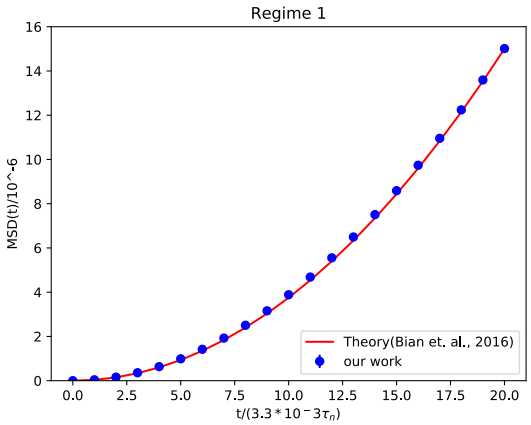

(a) Ballistic regime

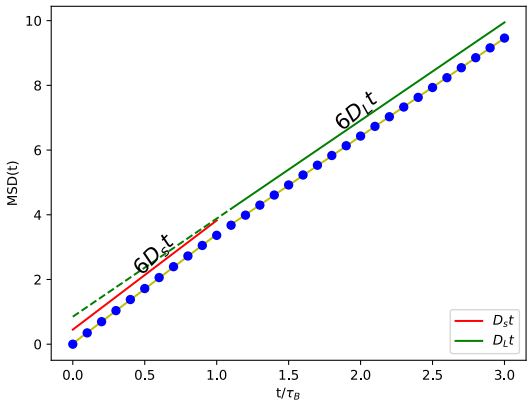

(b) Short-time and long-time self-diffusion regime

Fig.4 Mean square displacement of the three regimes with Gaussian-core potential model

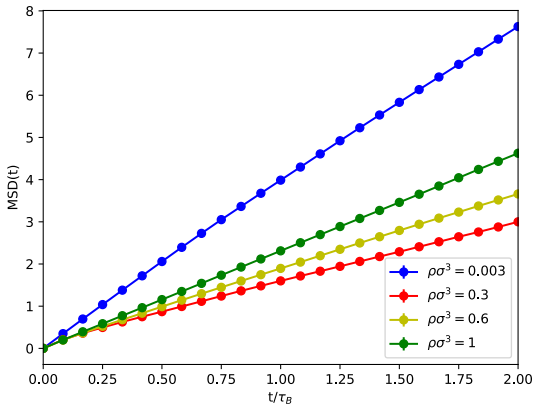

Fig.5 Mean square displacement of Gaussian-core potential model at $\rho\sigma^3$=0.003, 0.3, 0.6, 1.0

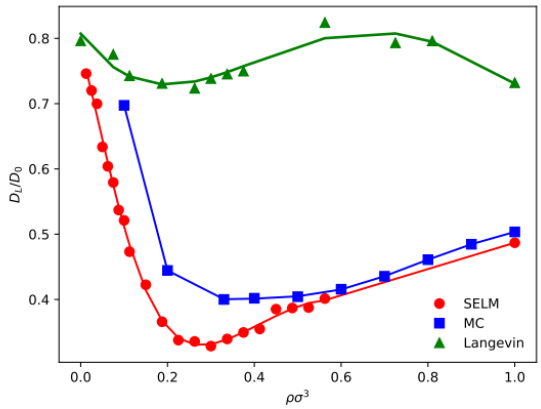

Fig. 6 Dimensionless density $\rho\sigma^3$ dependence of long-time self-diffusion coefficients D_L/D_0 for a suspension of soft-spherical particles

4. Conclusions

In summary, we have studied the short-time and long-time self-diffusion of the spherical particles at different volume fractions through two models with the *WCA* and the Gaussian-core potential respectively by using the SELM method which takes into account both hydrodynamic and Brownian effects. The diffusion of the particle at finite concentration described by three time regimes is confirmed. The relationship between the self-diffusion coefficient and the volume fraction is obtained and shows different features. For *WCA* potential model, the diffusion coefficient decreases monotonically with the increase of the volume fraction, while for Gauss-core potential model, the diffusion coefficient decreases initially, and reaches its minimum at $\rho\sigma^3$=0.3, it then turns to increase with increase of the volume fraction and regains about 50% from its minimum at $\rho\sigma^3$=1.0. The SELM method is also suitable to study the hydrodynamic properties of polymers (L-shape, rod-like, dumbbell) [39-43]. Furthermore, the method can be extent to study the hydrodynamic properties of active particles and charged particles by adding an external force or Coulomb potential.

Funding information This work was financially supported by the National Natural Science Foundation of China (11601381).

Compliance with ethical standards

Conflict of interest The authors declare that they have no conflict of interest.

References

1. Yu M, Qiao X, Dong X, Sun K(2018) Shear thickening effect of the suspensions of silica nanoparticles in PEG with different particle size, concentration and shear. Colloid Polym. Sci.296(8):1-8
2. Louis AA, Bolhuis PG, Hansen JP, Meijer EJ(2000) Can polymer coils be modelled as ”soft colloids”? Phys. Rev. Lett.85(12):2522– 2525
3. Likos CN, Rosenfeldt S, Dingenouts N, Ballauff M, Lindner P, Werner N, Vögtle F(2002) Gaussian effective interaction between flexible dendrimers of fourth generation: A theoretical and experimental study. J. Chem. Phys.117(4):1869–1877
4. GöTze IO, Harreis HM, Likos CN(2004) Tunable effective interactions between dendritic macromolecules. J. Chem. Phys.120(16):7761–7771
5. Federica LV, Leonid Y, Egorov SA, Kurt B(2011) Interactions between polymer brush-coated spherical nanoparticles: the good solvent case. J. Chem. Phys.135(21):214902
6. Kroeger A, Zhang B, Rosenauer C, Schlüter AD, Wegner C(2013) Solvent induced phenomena in a dendronized linear polymer. Colloid Polym. Sci. 291(12):2879–2892
7. Bülow S von, Siggel M, Linke M, Hummer G(2019) Dynamic cluster formation determines viscosity and diffusion in dense protein solutions. Proc. Natl. Acad. Sci. U.S.A.116(20):9843-9852
8. Benke M, Shapiro E, Drikakis D(2008) An efficient multi-scale modelling approach for ssdna motion in fluid flow. J. Bionic Eng.5(4):299–307
9. Napoli M, Atzberger P, Pennathur S(2011) Experimental study of the separation behaviour of nanoparticles in micro- and nanochannels. Microfluid. Nanofluid.10(1):69–80
10. Ottewill RH, Williams NSJ(1987) Study of particle motion in concentrated dispersions by tracer diffusion. Nature 325:232–234
11. Cheng Z, Zhu J ,Chaikin PM, See-Eng P, Russel WB(2002) Nature of the divergence in low shear viscosity of colloidal hard-sphere dispersions. Phys. Rev. E 65(4 Pt 1):041405
12. Beenakker CWJ, Mazur P(1983) Self-diffusion of spheres in a concentrated suspension. Physica A 126(3):349–370
13. Beenakker CWJ, Mazur P(1983) Diffusion of spheres in a concentrated suspension: Resummation of many-body hydrodynamic interactions. Phys. Lett. A 98(1):22–24
14. Hoh NJ, Zia RN(2016) Force-induced diffusion in suspensions of hydrodynamically interacting colloids. J. Fluid Mech.795:739– 783
15. Weeks JD, Chandler D, and Andersen HC(1971) Role of Repulsive Forces in Determining the Equilibrium Structure of Simple Liquids, J. Chem. Phys. 54, 5237
16. Baskaran A, Marchetti MC(2009) Statistical mechanics and hydrodynamics of bacterial suspensions. Proc. Natl. Acad. Sci. U.S.A. 106(37): 15567–15572
17. Lauga E(2016) Bacterial hydrodynamics. Annu. Rev. Fluid Mech. 48(1):105-130
18. Stillinger FH(1976) Phase transitions in the Gaussian core system. J. Chem. Phys.65(10):3968–3974
19. Shall LA, Egorov SA(2010) Structural and dynamical anomalies of a Gaussian core fluid: A mode-coupling theory study. J. Chem. Phys. 132(18):3968
20. Mausbach P, May HO(2006) Static and dynamic anomalies in the Gaussian core model liquid. Fluid Phase Equilib.249(1):17–23
21. Wensink HH, Löwen H, Rex M, Likos CN, Teeffelen S van(2008) Long-time self-diffusion for Brownian Gaussian-core particles. Comput. Phys.
22. Lang A, Likos CN, Watzlawek M, Löwen H(2000) Fluid and solid phases of the Gaussian core model. J. Phys.:Condens. Matt.12(24):5087–5108
23. Einstein A(1906) Zur theorie der brownschen bewegung. Ann. phys.324(2):371–381
24. Kovalchuk NM, Kuchin I, Starov V, Uriev N(2010) Aggregation in colloidal suspensions and its influence on the suspension viscosity. Colloid J. 72(3):379–388
25. Segrè PN, Behrend OP, Pusey PN(1995)Short-time Brownian motion in colloidal suspensions: Experiment and simulation. Phys. Rev. E 52(5): 5070–5083
26. Heinen M, Banchio AJ, NäGele G(2011) Short-time rheology and diffusion in suspensions of yukawa type colloidal particles. J. Chem. Phys. 135(15):5460–2324
27. Banchio AJ, Heinen H, Holmqvist P, Näqele G(2017) Short- and long-time diffusion and dynamic scaling in suspensions of charged colloidal particles. J. Chem. Phys.148(13):134902
28. Ando T, Skolnick J(2010) Crowding and hydrodynamic interactions likely dominate in vivo macromolecular motion. Proc. Natl. Acad. Sci. U.S.A.107(43):18457-18462.
29. Malevanets A, Kapral R(1999) Mesoscopic model for solvent dynamics. J. Chem. Phys.110(17):8605-8613
30. Brady JF, Bossis G(1988) Stokesian dynamics. Annu. Rev. Fluid Mech.20(1):111-157
31. Groot RD, Warren PB(1997) Dissipative particle dynamics: Bridging the gap between atomistic and mesoscopic simulation. J. Chem. Phys. 107(11):4423-4435
32. Goddard BD, Nold A, Kalliadasis S(2013) Multi-species dynamical density functional theory. J. Chem. Phys.138(14):14490
33. Wang Y, Sigurdsson JK, Atzberger PJ(2016) Fluctuating hydrodynamics methods for dynamic coarse-grained implicit-solvent simulations in lammps. Siam J. Sci. Comput.8(5):S62–S77
34. Plimpton S(1995) Fast parallel algorithms for short range molecular dynamics. J. Comput. Phys. 117(1): 1–19

35. Peskin CS(2002) The immersed boundary method. Acta Numer.11:479–517
36. Atzberger PJ(2011) Stochastic Eulerian Lagrangian methods for fluid-structure interactions with thermal fluctuations. J. Comput. Phys.230(8):2821–2837
37. Bian X, Kim C, Karniadakis G Em(2016) 111 years of Brownian motion. Soft Matter12:6331–6346
38. Phillips RJ, Brady JF, Bossis G(1988) Hydro-dynamic transport properties of hard-sphere dispersions. i. suspensions of freely mobile particles. Phys. Fluids31(12):3462–3472
39. Kümmel F, ten Hagen B, Wittkowski R, Buttinoni , Eichhorn R, Volpe G, Löwen H, Bechinger C(2013) Circular motion of asymmetric self-propelling particles. Phys. Rev. Lett.110(19):198302
40. Schwarz-Linek J, Valeriani C, Cacciuto A, Cates ME, Marenduzzo D, Morozov AN, and Poon WCK(2012) Phase separation and rotor self-assembly in active particle suspensions. Proc. Natl. Acad. Sci. U.S.A.109(11):4052–4057
41. Peruani F, Deutsch A, Bär M(2006) Nonequilibrium clustering of self-propelled rods. Phys. Rev. E 74(1):030904
42. Pham-Van H, Luc-Huy H, Nguyen-Minh T(2018) Templat-assisted assembly of asymmetric colloidal dumbbells into desirable cluster structures. Colloid Polym. Sci.296(8):1387–1394
43. Park BS, Jung KI, Lee SJ, Lee KY, Jung HW(2018) Effect of particle shape on drying dynamics in suspension drops using multi-speckle diffusing wave spectroscopy. Colloid Polym. Sci.296(5):971-979